Defense Threat Reduction Agency
8725 John J. Kingman Road, Stop 6201
Fort Belvoir, VA 22060-6201

DTRA-TR-24-06

FINAL REPORT

KeV High Harmonic Generation Enhanced by Mid-IR Surface Plasmon

15 December 2023

PI: Dr. Zenghu Chang

The University of Central Florida

REPORT DOCUMENTATION PAGE

1. REPORT DATE	2. REPORT TYPE	3. DATES COVERED	
		START DATE	END DATE
20231215	Final Grant Report	20200201	20230731

4. TITLE AND SUBTITLE

KeV High Harmonic Generation Enhanced by Mid-IR Surface Plasmon

5a. CONTRACT NUMBER	5b. GRANT NUMBER	5c. PROGRAM ELEMENT NUMBER
	HDTRA11910026	
5d. PROJECT NUMBER	**5e. TASK NUMBER**	**5f. WORK UNIT NUMBER**

6. AUTHOR(S)

Chang, Zenghu; Corkum, Paul.

7. PERFORMING ORGANIZATION NAME(S) AND ADDRESS(ES)

University of Central Florida (P.O. Box 160000, Orlando, FL 32816, USA).
Joint Attosecond Science Laboratory, University of Ottawa (550 Cumberland St, Ottawa, ON, K1N 6N5 Canada) and National Research Council of Canada

8. PERFORMING ORGANIZATION REPORT NUMBER

9. SPONSORING/MONITORING AGENCY NAME(S) AND ADDRESS(ES)	10. SPONSOR/MONITOR'S ACRONYM(S)	11. SPONSOR/MONITOR'S REPORT NUMBER(S)
Defense Threat Reduction Agency/RD-NTS 8725 John J. Kingman Rd., MSC 6201 Ft. Belvoir, VA 22060-6201	DTRA/RD-NTS	DTRA-TR-24-06

12. DISTRIBUTION/AVAILABILITY STATEMENT

Cleared for Public Release

13. SUPPLEMENTARY NOTES

14. ABSTRACT

Effects of enhancement of short-wavelength infrared intense laser field in a single micrometer-scale metal funnel were observed for the first time in harmonic generation experiments. Low-order harmonics were generated by interesting 32-femtosecond pulses centered at 2.2-micron wavelength with gases in the funnel. The driving laser was an optical parametric amplifier operating at 60-kilohertz repetition rate. When the peak intensity of the laser beam at the entry of the funnel reached 9.1 terawatt (TW) per square centimeter, third harmonic signals were detected with an estimated enhancement factor of 6.2. At a higher intensity, 49 TW per square centimeter, the enhancement of the fifth harmonic was demonstrated. The results paved the way for generating high-order harmonics at high repetition rate with microjoule-level driving lasers.

15. SUBJECT TERMS

harmonic generation, laser optics, pulse laser

16. SECURITY CLASSIFICATION OF:			17. LIMITATION OF ABSTRACT	18. NUMBER OF PAGES
a. REPORT	b. ABSTRACT	C. THIS PAGE		
Unclassified	Unclassified	Unclassified	Unclassified	11

PREVIOUS EDITION IS OBSOLETE.

STANDARD FORM 298 (REV. 5/2020)
Prescribed by ANSI Std. Z39.18

19a. NAME OF RESPONSIBLE PERSON	19b. PHONE NUMBER *(Include area code)*
Jacob Calkins	(510) 616-4033

DTRA Basic Research Final Report

Grant/Award #: HDTRA11910026

PI Name: Zenghu Chang

Organization/Institution: University of Central Florida

Project Title: KeV High Harmonic Generation Enhanced by Mid-IR Surface Plasmon

Abstract

Effects of enhancement of short-wavelength infrared intense laser field in a single micrometer-scale metal funnel were observed for the first time in harmonic generation experiments. Low-order harmonics were generated by interesting 32-femtosecond pulses centered at 2.2-micron wavelength with gases in the funnel. The driving laser was an optical parametric amplifier operating at 60-kilohertz repetition rate. When the peak intensity of the laser beam at the entry of the funnel reached 9.1 terawatt (TW) per square centimeter, third harmonic signals were detected with an estimated enhancement factor of 6.2. At a higher intensity, 49 TW per square centimeter, the enhancement of the fifth harmonic was demonstrated. The results paved the way for generating high-order harmonics at high repetition rate with microjoule-level driving lasers.

1. Introduction

High-order harmonic generation (HHG) [1, 2] is a well-developed coherent extreme ultraviolet (XUV) and soft X-ray source for probing electron dynamics in atoms, molecules, and condensed matter [3-7]. Many efforts have been devoted to increase the repetition rate of the light sources from kHz to MHz, which aimed at significantly decreasing the data accumulation time of time-resolved photoelectron spectroscopy experiments. Several approaches have been demonstrated to generate coherent vacuum UV and XUV pulses at MHz level, including HHG driven by fiber and thin-disk lasers [8-10], as well as in enhancement cavities [11-14].

Recently plasmonic HHG has attracts interest because the required laser energy is very low. It takes advantages of electric field enhancement by the surface plasmonic polariton (SPP) when a femtosecond laser pulse propagates along the metal/dielectric interface in a metallic nanostructure [15]. In 2011, I. Park *et al.* experimentally observed an enhancement factor of 350 in a nanoscale funnel structure. XUV pulses down to 18.6 nm were generated in Xenon gas [16]. The authors focused 800-nm, 10-fs laser pulses at 75 MHz into a silver funnel nanostructure and generated up to the 43rd harmonics in Xenon gas. They also compared the results between funnel and bow-tie structures and claimed that the former has higher thermal immunity. Its larger interaction volume improved the HHG efficiency [22]. In 2012, M. F. Ciappina *et al.* theoretically predicted that the inhomogeneous electric field in gold bow-tie structures has important effect on HHG and results in an extension of harmonic cutoff [17]. Furthermore, S. Han compared the plasmon-enhanced HHG from Al_2O_3 cone structures with and without gold coating. The author found that the HHG from the Al_2O_3 cone structure without gold coating is less efficient but has a longer lifetime than the coated structure [24]. In 2016, S. Han *et al.* have fabricated a metal-sapphire funnel structure and observed an intensity enhancement up to 20 dB with 800-nm, 12-fs laser pulses at 75 MHz. Harmonics signals at 60 nm were detected. By merging nano technology and attosecond physics,

HHG enhanced by surface plasmon has wide applications, including isolated attosecond pulse generation, nanoscale near field sampling, and nanoscale microscopy [18-20].

Although significant progress has been made in plasmon-enhanced HHG research, several issues need to be resolved to make such XUV sources competitive. Firstly, the metal structure can be damaged by the femtosecond laser pulses. Secondly, the energy conversion efficiency is very low. Thirdly, incoherent atomic emission lines exist in the spectrum [21]. In some experiments, only incoherent fluorescent emission was observed from argon in bow-tie structures at 15 bar backing pressure [23]. Therefore, the mechanism of plasmonic harmonics from the gas in the metallic nanostructures are still under debate.

Previous HHG experiments in enhanced field were conducted with near infrared lasers. In this DTRA funded program, effects of enhanced electric field of a 2.2-μm laser in a metallic funnel structure on harmonic generation in gases were observed for the first time to the best of our knowledge. There are potential advantages to drive HHG in gas filled funnels by the short-wave infrared (SWIR) laser pulses. With the lower photon energy of the driving laser, metals can withstand higher laser intensity. Meanwhile, the longer the driving wavelength, the larger the funnel structure size, where more gas atoms exist in the nanostructures for a given pressure. In addition, for SWIR laser, thicker metal foil can be used to fabricate nanostructures, which may allow a higher gas pressure to increase the photon flux of the harmonics.

2. Materials and Methods

2.1 Sample fabrication and numerical simulations of laser field enhancement

The scheme of generating high harmonics in a micrometer-scale gold funnel with LWIR laser is depicted in Fig. 1 (a). The laser beam enters the funnel from the large diameter opening. The laser field is enhanced by the surface plasmon as it propagates awards the small-diameter exit. Finite-difference time-domain (FDTD) calculations using commercial software (Lumerical FDTD Solutions; Ansys) were performed to compare the SWIR intensity enhancement in two different structures. The gold funnel structure was assumed to be a truncated cone, as illustrated in Figure 1 (a). The incident laser was a 2.2-micron few-cycle pulse with a pulse width of 32 fs. The pulse shape was Gaussian, and the waist radius was 6.5 micron. It started from the bottom of the funnel structure and propagated along the z-axis. The polarization direction was parallel to the x-axis. For calculation, the mesh was set to 25 nm×25 nm ×25 nm under perfectly matched layer boundary conditions.

Fig. 1 (a) and (b) show the enhanced intensity distribution in the xz plane. The intensity enhancement factors have an enormous value at the Au-vacuum interface around the apex of both funnel structures. The maximum intensity enhancement factors were 43.4 and 75.2 for structures with inlet diameters of 15 and 10 micron, respectively. The intensity enhancement formed inside the funnel structures has periodicity along the x-axis. It shows that the overlap between the internally reflected and incident pulses contributes to the intensity enhancement inside the structure. Gold funnel structures were fabricated by focused ion beam milling. Electron microscope images of the cross sections of two funnel structures are shown in Fig. 1(c) and (d).

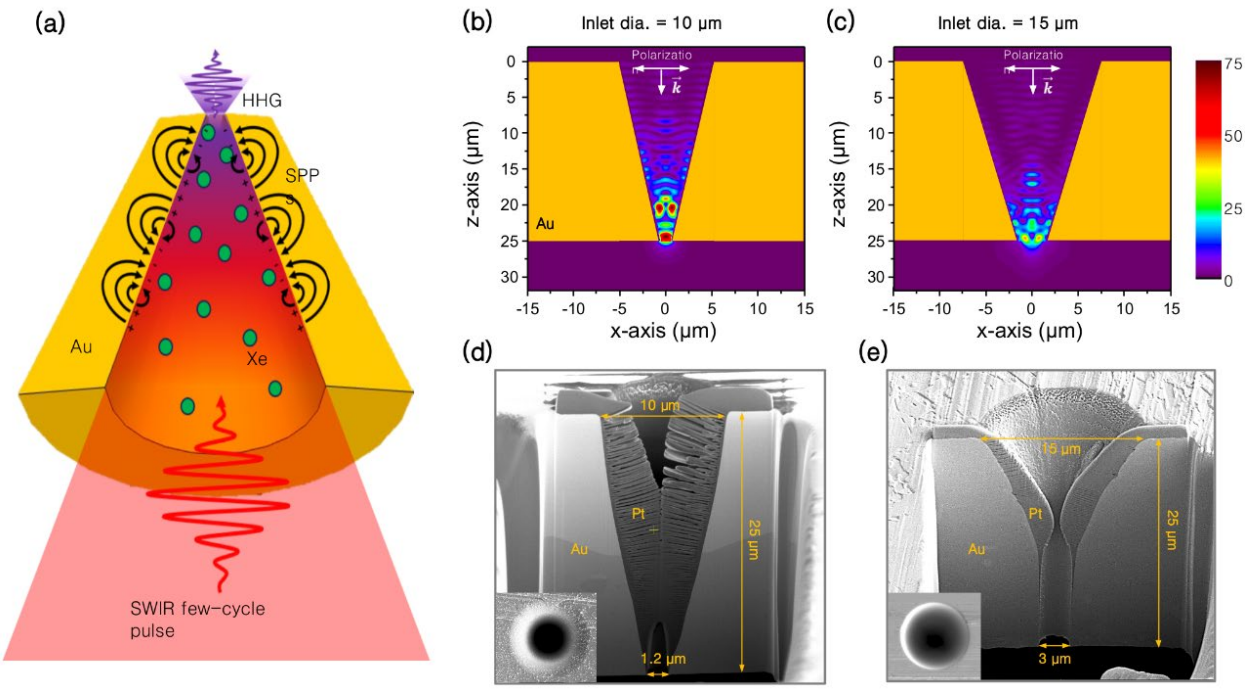

Fig. 1. (a) The principle of high harmonic generation in a metal funnel. The calculated SWIR intensity enhancement in two different structures: (b) input diameter of 15 micron and outlet diameter of 3 micron; (c) input diameter of 10 micron and outlet diameter of 1 micron. The laser beam propagates from the bottom to the top. (d) and (e) Electron microscope images of the cross sections of two funnel structures. Inserts are the top views. The Pt layers are just obtaining the images. They do not exist in harmonic generation experiments.

Funnels (or pyramids) were created in Ottawa by a focused ion beam. Silicon was chosen assuming that it was the most studied material that allowed the best fabrication and pyramids because they were easier to image. Figure 2 shows a simulation of a silicon pillar. The simulation shows that it is possible to place the interference maximum on the surface and that the field enhancement could exceed 10. Having peak field at the surface is especially important with pyramids since the harmonics are easily absorbed by the material in which the harmonics are generated. Figure 3 shows one of the better cones that we have constructed. It was noticed that the apex is not flat, often the side walls are not straight, the bottom has a large modulation, and the dimensions are only approximately achieved. The problem is that the large depth of material that must be removed requires a high energy gallium beam. The fabrication challenges are under investigation.

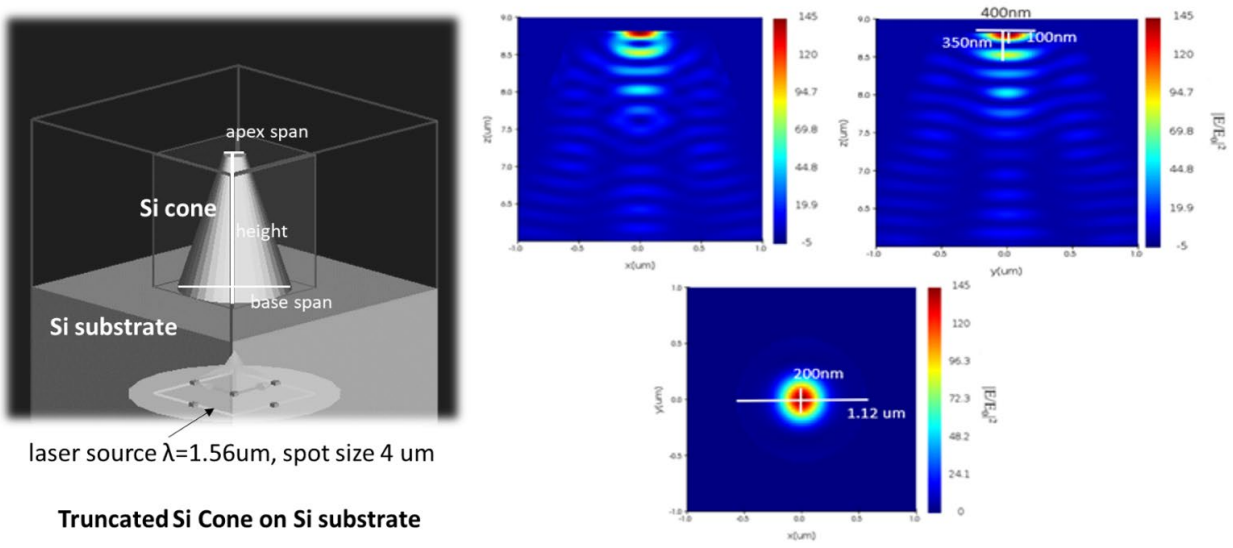

Fig 2. Left is a simulated Silicone pyramid, while right is a simulation of the field strength where the interference maximum was placed at the exit face of the pyramid. Note the field increase is more than a factor of 10.

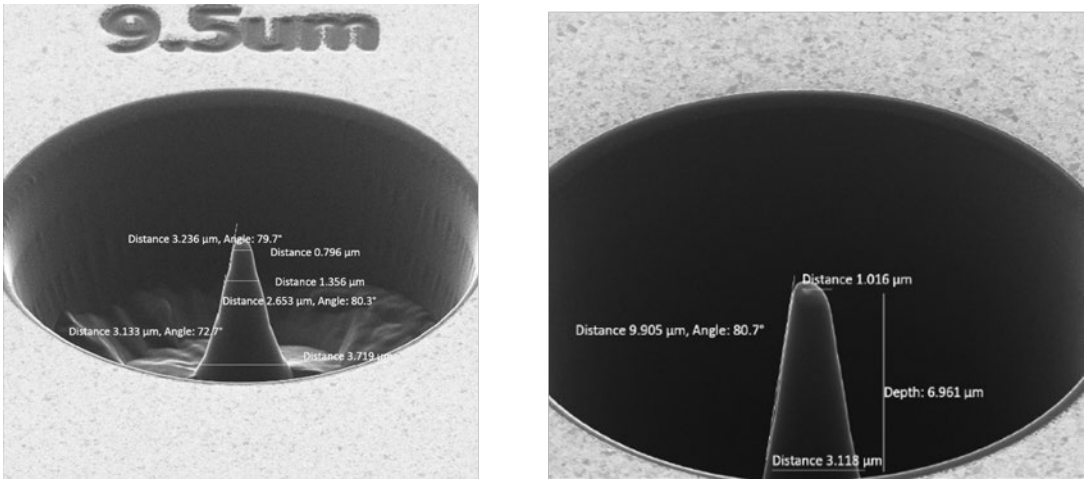

Fig. 3. Electron microscope images of cone structures that were fabricated from silicon aiming for the dimensions that modeled in Figure 2.

2.2 Harmonic generation setup

The experimental setup for harmonic generation in gas filled micrometer-scale funnels is shown in Fig.4 (a). A commercial optical parametric amplifier (OPA) pumped by a Yb-laser (Light-conversion) delivers 2.2-µm pulses with energy up to 2 µJ at a repetition rate of 60 kHz. The output beam was focused to mental funnels filled with gas to generate harmonics. The funnel structure was fabricated on a thin gold foil with focused ion beams. The thickness of the gold foils is 25 µm. Two different sizes of funnel structures are used. One with an input diameter of 15 µm and an outlet diameter of 3 µm, and the other with an input diameter of 10 µm and an outlet diameter of 1 µm. The funnel structure was mounted on a three-dimensional pico-motor stage in a vacuum chamber filled with Xeon gas.

The spectrum of the OPA output is shown in Fig. 4 (b). The 318-nm FWHM corresponds to a Fourier-transform limited pulse duration of 22.3 fs. The negative chirp of the pulses was compensated by ZnSe windows that resulted in 32-fs pulses, as shown in Fig 4 (c). To couple the SWIR beam into the micrometer size funnel structure, an *f*=12.7 mm, AR-coated ZnSe lens was used to focus the laser beam. The measured radius of laser beam at the focus was 7.4 micron, as shown in Fig. 4 (d) and (e).

A major challenge was how to focus the invisible SWIR beam into a single funnel structure with diameter of about 15 μm. To visualize the funnel structure, a He-Ne laser copropagating with the SWIR beam was added to the system, as depicted in Fig. 4 (a). The funnel sample was imaged by the combination of two lenses with 12.7-mm and 500-mm focal lengths respectively. The image was further magnified by a 10× microscope objective, which could be seen on by eyes a white paper. During the experiments, a pen marking on the substrate of the tunnel was first imaged by the He-Ne laser with a total magnification about 100. Then the funnel structures were imaged by translating the sample perpendicular to the laser propagation direction. Finally, the sample was moved to the laser focus to make sure only a single funnel structure was imaged by the He-Ne laser. The funnel structure was fine-tuned by checking the transmitted 2.2-micron laser with an infrared camera. The harmonic beam generated from the xenon gas was collimated and focused by two off-axis parabolic mirrors into a spectrometer.

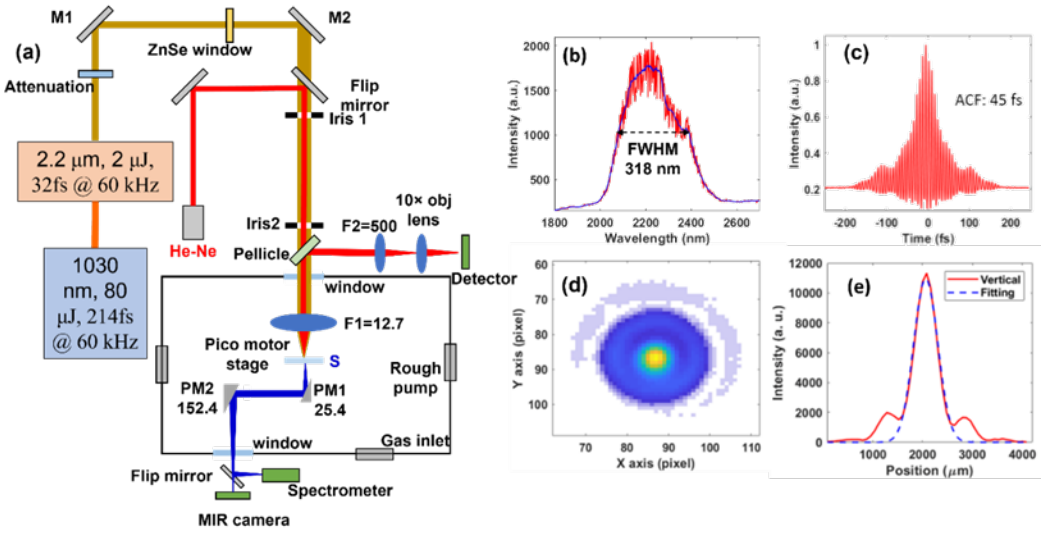

Fig. 4. Experimental setup for harmonic generation in a gas filled funnel and the properties of the SWIR laser.

3. Results and Discussion

Third harmonic generation experiments were conducted under three different target conditions for a comparison: (1) free space filled with xenon gas (not funnel structures), (2) no gas in 10-micron diameter funnels, and (3) xenon gas-filled funnels. The gas pressure can be changed set at 49 torr. The peak intensity at the SWIR laser focus was set to 9.1 TW per square centimeter, which is also the intensity at the entry of the funnel. The results are shown in Fig. 5 (a). No third harmonic signal was detected, because the laser intensity is too low to ionize xenon gas. When the funnel structure

was placed at the focal point of the laser beam, the third harmonic signal was much stronger at 49 torr than at 0 torr because of the interaction between the enhanced laser field and Xe atoms. The weak signal at 0 torr was from surface harmonic generation.

The third harmonic signal is proportional to the square of gas pressure inside the 10-micron diameter funnel changes from 0 to 50 torr. After that the signal starts to decrease until 100 torr, then the signal hardly changes with gas pressure, as shown in Fig. 5 (b). Similar phenomenon was observed in the 15-micron diameter funnel structure, as shown in Fig. 5 (c). The quadratic pressure dependence below 50 torr is strong evidence that the nonlinear process is phase matched. The large difference between the harmonic signals with and without the funnel structure provides explicit evidence that the coherent third harmonic was generated in the enhanced laser field from the surface plasmon polariton.

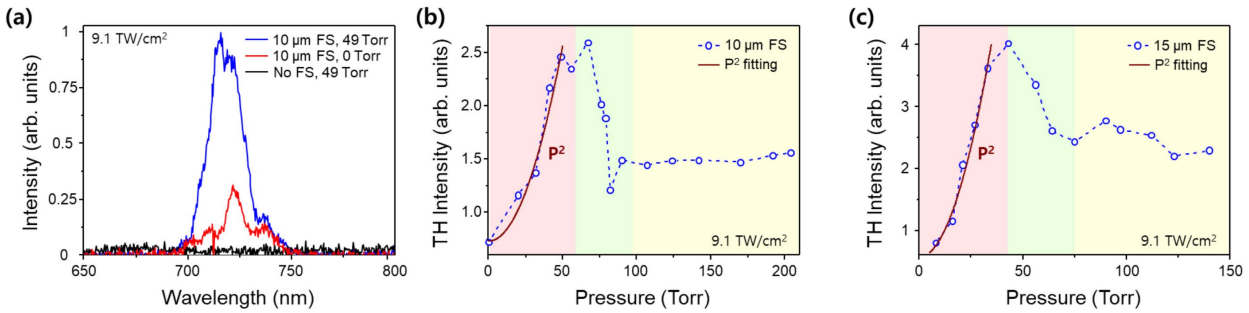

Fig. 5. Third harmonic generation in xenon gas driven by the 2.2-micron laser under different conditions. (a) with and without the funnel structure. (b) with the 10-micron diameter funnel target. (c) with the 15-micron diameter funnel target.

The third harmonic signals in the 10-micron diameter funnel structure were measured when the peak intensity was increased from 5.7 to 10.2 TW per square centimeter at given Xe pressures. The strength of the signal was proportional to the third power of the intensity as shown in Fig. 6 (a). When the peak intensity reached 11.4 TW per square centimeter, the signal started to deviate from the cubit curve, which indicates that the funnel structure suffered from laser induced damage. The intensity is consistent with the measured damage threshold. Similar results were observed with the 15-micron diameter funnel structure, as shown in Fig. 6 (b).

When the peak intensity reached 49 TW per square centimeter, fifth harmonic was observed with the 10-micron diameter funnel structures, as shown in the red curve in Fig. 6 (c). As a comparison, the harmonic spectrum without funnel structure is shown as blue curve at the same laser intensity. Our results clearly showed that there is still field enhancement effect even when damaging exists in the funnel structures.

To estimate the field enhancement factor with the funnel structures, third harmonics were generated when the funnels were moved away from the laser beam. By extrapolating the results obtained without using the funnel and compared with that with the funnel, an enhancement factor is 6.2 were obtained. The field enhancement factor is smaller than the predictions of the simulations due to the smaller number of atoms contained in the funnel structure than that in the focal volume is free space.

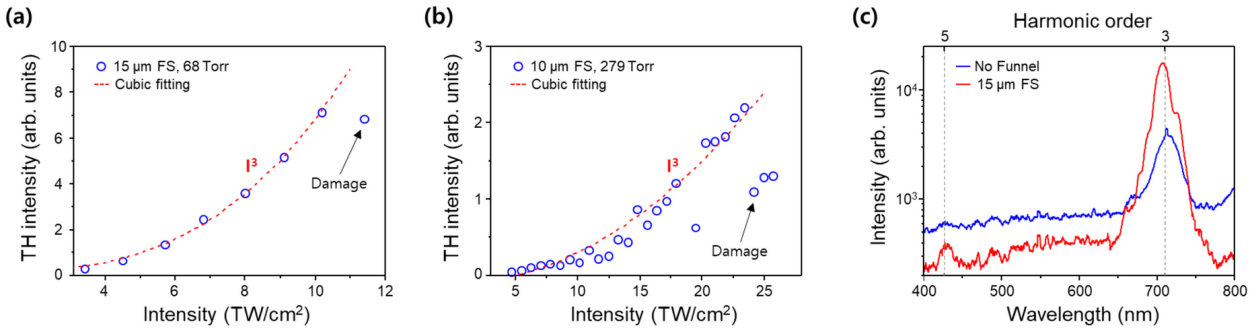

Fig. 6. Intensity-dependence of the 3rd harmonic generation in Xenon gas in the 10-micron (a) and 15-micron (b) diameter funnel structures driven by the 2.2-micron laser. (c) Observation of enhanced 5th harmonic generation at 49 TW per square cm from the 15-micron diameter funnel structure.

Figure 7 illustrates the deformed funnel structures following the irradiation of the few-cycle SWIR laser pulses. The material damage to the metal film can be attributed to a thermal process, wherein melting and ablation occur upon reaching a critical energy density. In the femtosecond time domain, energy deposition is primarily governed by electron absorption and subsequent hot electron diffusion. For films thinner than the penetration depth of pulse energy into the material, the damage threshold exhibits a linear relationship with film thickness. Conversely, for films thicker than the penetration depth, the ablation threshold remains constant at its bulk value. Given that the penetration depth of gold is approximately 180 nm, the fabricated funnel structures can be considered in a bulk state. The damage threshold of bulk gold is known to be 0.4 Jule per square cm with multiple femtosecond pulse exposures. In these experiments, the laser fluence applied, approximately 0.3 Jule per square cm based on a case of 10 TW per square cm, falls below the damage threshold of bulk gold. Consequently, the deformation of the funnel structures is attributed to the amplified laser field generated by field enhancement within the plasmonic structures. However, it appears that internal structural deformation occurs due to melting, vaporization, and re-deposition of gold caused by the enhanced laser field, leading to a reduction in the field enhancement effect for the high harmonic generation.

Compared to gold that is a fragile metal, TiN is a hard, refractory material with a very high melting point. It is often used by carpenters to form a hard surface on drills or other tools, as a gold-colored affordable material on monumental buildings and as an indestructible surface for household tools such as irons. TiN epitaxially grown on MgO was obtained through a collaboration with a Perdue group. Silver epitaxially grown in silicon is another interesting material for a comparison. One might expect that the TiN will not damage easily whereas the silver may. It was discovered experimentally that in both cases the damage threshold is so high that high harmonics were produced at the approximate efficiency of a highly efficient transparent substrate. *These are the first reported observations of high harmonics from metals*.

Figure 8 illustrates the damage threshold of TiN on MgO and silver on silicon. At 3.5 x 10^{13} W/cm^2 the damage threshold for silver on Silicon (right dashed line) is consistent with efficient production of high harmonics from Xenon with photon energy exceeding 100 eV if a mid-infrared

pulse were used. Furthermore, it is expected that a higher damage threshold for metals when high intensity infrared light replaces the 800-nm light used in this experiment.

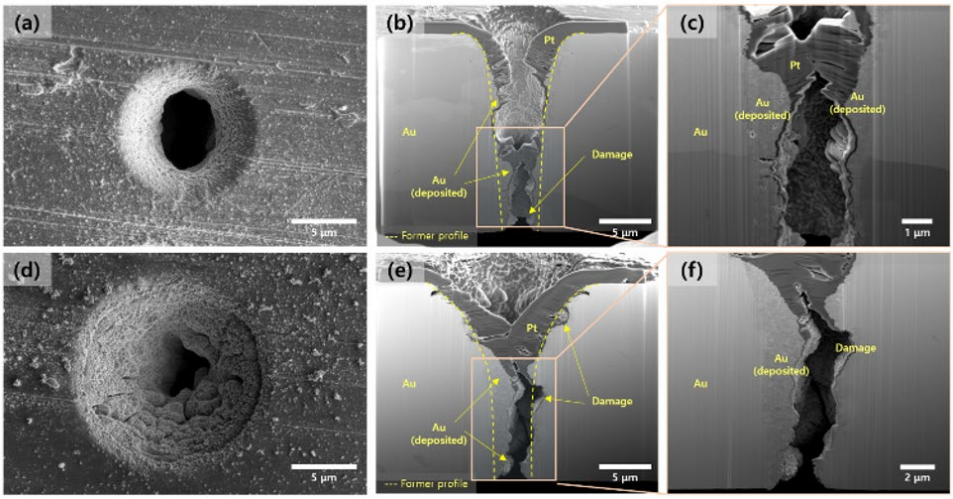

Fig. 7. SEM images of the funnels after exposure to the SWIR laser pulses. (a) Top-view image showing the 10-micron diameter funnel inlet. (b) Cross-sectional view of the 10-micron funnel. (c) Enlarged cross-section of the 10-micron funnel. (d) Top-view image depicting the 15-micron diameter funnel inlet. (e) Cross-sectional view of the 15-micron funnel. (f) Enlarged cross section of the 15-micron funnel.

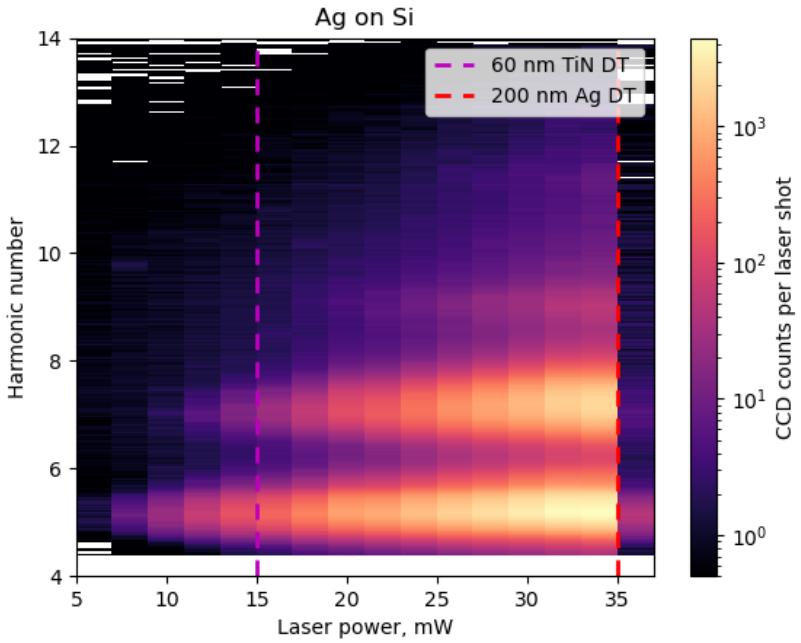

Fig. 8. We show the damage threshold for multi-shot damage of TiN with the pink dashed line at 15 mW (I=1.5 x 10^{13} W/cm^2) and for Ag on silicon at 35 mW (I=3.5 x 10^{13} W/cm^2). We have used a kHz laser producing a few-cycle pulse of 800 nm radiation and below the dashed lines we observe no damage even after more than 10^5 shots. The horizontal data shows the harmonic number for different pulse energies for Ag on silicon. At 200 nm thick, the harmonics are from silver.

4. Conclusions and outlook

The effects of enhanced laser field on harmonic generation in gas-filled single metal funnel structures with 2.2-micron driving laser were observed for the first time, to the best of our knowledge. The third and fifth harmonic were observed at the input intensity of 9.1 TW per square cm. The maximum enhancement was estimated to be 6.2. The results show a potential way to generate coherent XUV source at high repetition rates. In future, materials with higher damage threshold may be used to fabricate the funnels to generate high order harmonics.

It is recommended to test TiN, silver and other metals with mid-infrared (4-10 μm). Using the best knowledge so far, it is recommended that nano/micro-funnels be made from single crystal silver. It is proposed the fundamental radiation be a mid-infrared beam since some improvement in the damage threshold by using IR radiation is expected. It is further recommended that Xenon be used as a target (preferably solid or liquid Xenon with nano-funnels), to reach the highest density possible, consistent with high harmonics. It is also suggested that the nano/micro-funnels have some transmission to allow partial phase matching, (as has been seen with counter propagation beams [25]).

However, there is another approach. One can use a thin layer of rare-gas solid or liquid on a pre-shaped, low NA substrate such as MgO or quartz. The substrate is a template that allows the harmonics to focus to a small high-resolution spot. Since either metals or dielectrics can form possible substrates, there is a larger pallet of materials to choose from. The first step in making efficient harmonics lies with high damage threshold materials irradiated with mid-IR light and relatively low density, rare gas liquids or solids. The required high repetition rate intense MIR driving lasers are available to the collaborating team of the Drs. Chang and Corkum [26, 27].

5. References

[1] E. Priori, G. Cerullo, M. Nisoli, S. Stagira, and S. De Silvestri, P. Villoresi, L. Poletto, and P. Ceccherini, C. Altucci, R. Bruzzese and C. de Lisio, Phys. Rev. A. 2000; 61: 063801.

[2] L F. Wang, X K. He, H. Teng, C X. Yun, W. Zhang, and Z-Y, Wei, Appl. Phys. B. 2015; 121: 81.

[3] F. Krausz, and M. Ivanov, Rev. Mod. Phys. 2009; 81: 163.

[4] N. Saito, H. Sannohe, N. Ishii, T. Kanai, N. Kosugi, Y. Wu, A. Chew, S. Han, Z-H. Chang, and J. Itatani, Optica. 2019; 6: 1542.

[5] A. Chew, N. Douguet, C. Cariker, J. Li, E. Lindroth et al., Phys. Rev. A. 2018; 97: 013407 (R).

[6] J. Li, J. Lu, A. Chew, S. Han, J-L. Li, Y. Wu, H. Wang, S. Ghimire, and Z-H. Chang, Nat. Commun. 2020; 11: 2748.

[7] S. Han, K. Zhao, and Z. Chang, Sensors. 2022; 22: 7513.

[8] D. Couch, D. Hickstein, D. Winters, S. Backus, M. Kirchner, S. Domingue, J. Ramirez, C. Durfee, M. Murnane, and H. Kapteyn, Optica. 2020; 7: 832.

[9] J. Fischer, J. Drs, F. Labaye, N. Modsching, V. Wittwer, and T. Südmeyer, Opt. Express. 2021; 29: 5833.

[10] M. Keunecke, C. Möller, D. Schmitt, H. Nolte, G. Matthijs, M. Reutzel, M. Gutberlet, G. Halasi, D. Steil, S. Steil, and S. Mathias, Rev. Sci. Instrum. 2020; 91: 063905.

[11] C-K. Zhang, S. B. Schoun, C. M. Heyl, G. Porat, M. Gaarde, and J. Ye, Phys. Rev. Lett. 2020; 125: 093902.

[12] J. Nauta, J-H. Oelmann, A. Borodin, A. Ackermann, P. Knauer, I. Muhammad, R. Pappenberger, T. Pfeifer, and J. Urrutia, Opt. Express. 2021; 29: 2624.

[13] A. Mills, S. Zhdanovich, M. X. Na, F. Boschini, E. Razzoli, M. Michiardi, A. Sheyerman, M. Schneider, T. Hammond, V. Süss, C. Felser, A. Damascelli, and D. Jones, Rev. Sci. Instrum. 2019; 90: 083001.

[14] T. Saule, S. Heinrich, J. Schötz, N. Lilienfein, M. Högner, O. deVries, M. Plötner, J. Weitenberg, D. Esser, J. Schulte, P. Russbueldt, J. Limpert, M. Kling, U. Kleineberg, and I. Pupeza, Nat. Commun. 2019; 10: 458.

[15] M. Stockman, Phys. Today. 2011; 64: 39–44.

[16] I. Park, S. Kim, J. Choi, D. Lee, Y. Kim, M. Kling, M. Stockman, and S. Kim, Nat. Photonics. 2011; 5: 677.

[17] M. F. Ciappina, S. S. Acimovic, T. Sharran, J. Biegert, R. Quidant, and M. Lewenstein, Opt. Express. 2012; 20: 26261.

[18] J. Choi, S. Kim, I-Y. Park, D-H. Lee, S. Han, and S-W. Kim, New. J. Phys. 2018; 14: 103032.

[19] B. Förg, J. Schötz, F. Sümann, M. Förster, M. Krüger, B. Ahn, W.A. Okell, K. Wintersperger, S. Zherebtsov, A. Guggenmos, V. Pervak, A. Kessel, S. A. Trushin, A. M. Azzeer, M. I. Stockman, D. Kim, F. Krausz, P. Hommelhoff, and M.F. Kling, Nat. Commun. 2016; 7: 11717.

[20] P. Dombi, and Z. Pápa, J. Vogelsang, S. V. Yalunin, M. Sivis, G. Herink, S. Schäfer, P. Groβ, C. Ropers, and C. Lienau, Rev. Mod. Phys. 2020; 92: 025003.

[21] M. Sivis, M. Duwe, B. Abel, and C. Ropers, Nat. Phys. 2013; 9: 304.

[22] I-Y. Park, J. Choi, D-H. Lee, S. Han, S. Kim, and S-W. Kim, Ann. Phys. (Berlin) 2013; 525: 87.

[23] S. Han, H, Kim, Y-W Kim, Y-J. Kim, S. Kim, I-Y. Park, and S-W. Kim, Nat. Commun. 2016; 7: 13105.

[24] S. Han, Photonics. 2022; 9: 427.

[25] A. Korobenko, T. J. Hammond, C. Zhang, A. Yu. Naumov, D. M. Villeneuve, and P. B. Corkum, "High-harmonic generation in solids driven by counter-propagating pulses", Optics Express, 2019; 27, 32630.

[26] Fangjie Zhou, Yi Wu, Alphonse Marra, Zenghu Chang, "Efficient generation of femtosecond millijoule pulses at 3.1 μm," Optics Letters, 2022; 47: 6057.

[27] Z. Alphonse Marra, Yi Wu, Fangjie Zhou, Zenghu Chang, "Cryogenically cooled Fe: ZnSe-

based chirped pulse amplifier at 4.07 μm," Optics Express, 2023; 31:13447.